

Revising the Goals and Means for the Base-to-Air Cooling Stage for Semiconductor Heat Removal - Experiments and Their Results

Travkin, V.S., Hu, K., Rizzi, M., Canino, M., and Catton, I.
 Department of Mechanical & Aerospace Engineering
 University of California, Los Angeles
 Box 951597, Los Angeles
 travkin@iname.com

Abstract

The development of simulation methods and data reduction for heat sink experiments are the purpose for this work. The study dealt with an experimental investigation of semiconductor heat sinks performance characteristics. The heat sinks were constructed of aluminum and consisted of an arrays of staggered pin fins and longitudinal fins. The cooling fluid was an air and the experiments were conducted with a porous medium Reynolds number ranging from 400 to 17000. A number of data reduction parameters and procedures were developed using scaling heterogeneous formulation by volume averaging theory (VAT). Analysed the basic homogeneous heat transfer performance features and shown insolvency of using conventional Nusselt numbers, homogeneous heat transfer rate and effectiveness parameter. Introduced and analysed heterogeneous upper scale heat transfer characteristics. Provided comparisons with other studies.

Keywords: semiconductor heat sink, experiment, data reduction, design, two-scale, heterogeneous medium, performance characteristics

Nomenclature

d_{por}	$=4\langle m \rangle / S_w$ characteristic length [m]
E_{eff1}	Effectiveness of heat transfer per unit volume [1/K]
f_f	Fanning friction factor of momentum resistance in the volume [-]
k_c	Conductivity coefficient of coolant [W/m K]
k_f	Conductivity coefficient of fluid phase [W/m K]
k_s	Conductivity coefficient of solid phase [W/m K]
h_r	Global heat transfer coefficient of the reference flat bottom plate with the same hydraulic resistance ζ
H_r	Heat transfer rate per unit volume per unit temperature difference [W/m ³ K]
L_x	Length of the heat sink in[m]
$\langle m \rangle$	Porosity [-]
Nu_w	Bottom wall Nusselt number [-]
P_p	Pumping power per unit of volume [W/m ³]
q_w	Heat flux through the bottom surface of the heat sink [W/m ²]

S_{all}	Internal surface [m ²]
S_w	Specific surface of internal volume (bottom surface not included) [1/m]
S_w^*	The overall specific surface per unit volume of heat exchange [1/m]
S_{wint}	Internal wetted surface minus bottom surface [m ²]
S_{wb}	Bottom wetted surface [m ²]
$T_a(x)$	Averaged temperature over vertical coordinate mass flow [K]
T_{bc}	Bulk temperature of the coolant [K]
T_{in}	Inlet temperature of the coolant [K]
T_{max}	Maximum temperature of the wall [K]
\tilde{U}	Averaged interstitial velocity [m/s]
α_w^*	Combined (averaged over the all internal plus bottom surfaces) heat transfer coefficient [W/m ² K]
$\bar{\alpha}_{int}$	Mean heat transfer coefficient in volume of heat sink (averaged over the internal surface) heat transfer coefficient [W/m ² K]
ζ	Normalized hydraulic resistance
Ω	Volume of the heat sink [m ³]
ρ_f	Density of the coolant fluid [kg/m ³]

Introduction

The primary goal in semiconductor heat sink design is simple. It is to increase the heat transfer while decreasing the momentum resistance as for regular closed type heat exchangers is the goal. Nevertheless, as soon as everyone agrees that the best way to achieve the maximum heat transfer rate within a particular volume of heat sink is through the introduction of additional heat exchanging elements (ribs or pins of different shape) the problem becomes a two scale heterogeneous volumetric heat exchanger design problem. The processes on the lower scale heat transport – in and around a single transfer element (rib, fin) no longer describe the heat transfer rate of the whole sink. At the same time, the formulation of the problem of a heat sink for a one-temperature, or even a two-temperature homogeneous medium does not involve or connect the local (lower scale) transport

characteristics determined by the morphology of the surface elements, directly to the performance of heat sink nor does it give guidance on how to improve the performance characteristics.

In our effort to tie the experimental characteristics of heat sink to the theoretical scaled (VAT) description and simulation of semiconductor base-to-air heat sinks, we came to the process of coupling of two-scale modeling and experiment for heat sink design. Most past work focused on the upper scale performance characteristics resulting in many efforts to measure the bulk heat transport rate and in modeling of numerous morphologies (see, for example, Andrews and Fletcher (1996), Bejan and Morega, (1993); Bejan, (1995); Fabbri (1999); Jubran, Hamdan, and Abdualh (1993); Kim and Kim (1999); You and Chang (1997), etc.). In many cases, the experimental was data reduced to the homogeneous device effectiveness:

$$E_{\text{eff3}} = \frac{\text{Nu}}{f_f \text{Re}^3},$$

where f_f is the momentum resistance in the volume, and Nu , f_f , and Re are to be constructed using only one geometric parameter. The two scale, VAT upper scale governing equations applicable to this problem, contain four additional descriptive terms in the momentum equation (for 1D turbulent equation), seven terms in the fluid temperature equation, and five additional terms in the solid phase (reflecting heat transport through ribs, pins) temperature equations (Gratton et al. 1996; Travkin and Catton, 1999; Travkin et al., 2000).

At the present time, only some basics known about developmental needs for VAT heat exchanger governing equations. Contrary to simulation numerical experiments, the physical experiment is usually much more restrictive in terms of the number of local experimental points that can be obtained. It is a problem to properly make local measurements and to relate the measurements within the volume of the heat exchange device to the results from simulations because the data point is a pint value and the simulation value is an average over a volume of finite size. In this modeling effort and experiment we attempt to deal with both using the two-scale approach.

Methods Used for Assessment of Heat Sink Performance and Comparison

We analyze effectiveness models by Andrews and Fletcher (1996), parameters by You and Chang (1997), Fabbri (1999), among others, in effort to reveal the positive features in them.

Andrews and Fletcher (1996), provide comparisons of a wide variety of heat enhancing technologies based on the parameter of heat transfer rate per unit volume per unit temperature difference ($S_{\text{all}} \bar{\alpha}_{\text{all}} / \Omega$) and pumping power per

$$\text{unit volume } \frac{P}{\Omega} \left[\frac{W}{m^3} \right] = \frac{\dot{m} \Delta P}{\rho_f \Omega}.$$

You and Chang (1997) calculated the local Nusselt number for the flat channel with rectangular pin fins via:

$$\text{Nu}_x(x) = \frac{h_w(x) D^*}{k_f} = \frac{D^*}{k_f (T_w(x) - T_a(x))} \times$$

$$\left(-\langle m \rangle^2 k_f \left(\frac{\partial T_f}{\partial y} \right)_w - \langle 1-m \rangle^2 k_s \left(\frac{\partial T_s}{\partial y} \right)_w \right)$$

$$D^* = d_{\text{por}} = \frac{4\langle m \rangle}{S_w},$$

$$h_w = \frac{q''(x)}{(T_w(x) - T_a(x))} = \frac{\left(-\langle m \rangle^2 k_f \left(\frac{\partial T_f}{\partial y} \right)_w - \langle 1-m \rangle^2 k_s \left(\frac{\partial T_s}{\partial y} \right)_w \right)}{(T_w(x) - T_a(x))},$$

where $T_a(x)$ is the velocity weighted cross-stream average air temperature:

$$T_a(x) = \frac{1}{\delta U} \int_0^\delta T_f(y) u(y) dy.$$

The average Nu over the length of the sample is

$$\text{Nu} = \frac{1}{L} \int_0^L \text{Nu}_x(x) dx, \quad \text{Re} = \langle m \rangle \text{Re}_{\text{por}} = \frac{\tilde{U} 4\langle m \rangle^2}{\nu S_w}.$$

This Nusselt number is not an internal surface Nu_{in} , because it is the flux determined by heat transport in both phases.

Among the results You and Chang (1997) obtained there is a note on p. 842 that indicates that: "It should be noted that the Nusselt number is not dependent on the applied wall heat flux." Fabbri (1999) calculated for the laminar regime Nu_c (equivalent) number in the flat channel with longitudinal rib fins using the following:

$$h = \frac{q''}{(T_{\text{max}} - T_{bc})}, \quad \text{Nu}_e = \frac{h(2H)}{k_c},$$

where T_{bc} is the bulk temperature of the coolant, T_{max} is the maximum temperature of the wall, q'' is the heat flux per unit of surface uniformly imposed on the flat side of the finned plate [W/m^2], and k_c is the coolant coefficient of conductivity. They choose to represent effectiveness of the fin morphology by

$$E_c = \frac{q''}{q_r''} = \frac{h}{h_r} = \frac{h}{2.692 k_c (\zeta)^{1/3} / H}$$

where h_r is the global heat transfer coefficient of the reference flat bottom plate with the same hydraulic resistance ζ . He choose to define the normalized hydraulic resistance ζ as:

$$\zeta = \frac{(H^2)}{(12\mu \tilde{U} \langle m \rangle)} \left(-\frac{dp}{dx} \right)$$

The two morphologies we were dealt in this study of heat sink design were researched numerous times based on conventional one scale heat transfer-fluid mechanics descriptions see, for example, among others the works by Bejan and Sciubba (1992), Bejan and Morega (1993), Bejan

(1995, 1999), Kim and Kim (1999), You and Chang (1997). The major problem with this approaches is that their formulations (and consecutive experimental or theoretical studies) are done on the lower scale (homogeneous) of description – but the answers have been sought for the upper scale – general scale of the heat transfer device. As we mentioned, this gives the gap between the formulations and the goals.

Thus, Bejan and Morega (1993) while comparing the pin fins and plate fins morphologies of heat exchanger in laminar regime could not come to a conclusion – which of the structures is the best and why? Their answers are given in terms of local descriptive characteristics as optimal pin fin diameter and local thermal conductance. Meanwhile, in the work published by Bejan (1999) recently, the approach named by author as “constructal theory” appeared to be the one which started the hierarchical scaling VAT many years ago (more than 30 actually) - “The optimization proceeds in a series of volume subsystems of increasing sizes (elemental volume, first construct, second construct. The shape of the volume and the relative thicknesses of the fins are optimized at each level of assembly.”

In the work of Kim and Kim (1999), based on the Vafai and Tien’s (1981) model for porous medium flow equation close to the present one for a laminar regime. The nondimensional set of convective heat transfer equations does not have the correspondence to morphological parameters of the problem so, the authors studied the influence of channel’s aspect ratio ($H/w_s = \alpha_s$, w_s is the channel width), and the ratio of effective conductivities set up in the problem on the profiles of velocity and temperature.

We are mostly interested, as in earlier studies by Travkin et al. (2000, 2001), in question of how the device behaves in experiments and in the corresponding mathematical simulation as a whole unit. At the same time we are not engaged into the balance studies conventional in the heat exchangers technology.

Heterogeneous VAT Based One Phase Analysis of Semiconductor Heat Sinks Experimental Data for Two Morphologies of Semiconductor Heat Sinks

Using the heterogeneous media simplified VAT performance models and characteristics for heat transfer in a flat channel with non-specified medium morphologies of heat transfer volumetric results in the following:

a) overall heat transfer rate per unit volume per unit temperature difference in the device

$$H_r = S_{all} \alpha_w^* / \Omega \left[\frac{W}{m^3 K} \right],$$

where S_{all} is the total internal surface, α_w^* is the combined (averaged over the all internal and bottom surfaces) heat transfer coefficient, and Ω is the volume of heat transfer; and

b) pumping power per unit volume of the sink P_p

$$P_p = \frac{P}{\Omega}, [W/m^3],$$

c) effectiveness parameter for the volume of the heat sink that results in

$$E_{eff} = H_r / P_p.$$

These characteristics’ formulae given above are the same as used for heat exchangers performance elsewhere. Using the two scale VAT approach their detailed mathematical formulations would be very different as disclosed below.

To calculate the above parameters one needs to find first the bulk (mean) Fanning friction factor f_f for the volume of the heat sink which can be assessed using formulae based on VAT for experimental measurements of pressure loss (see Travkin and Catton, 1998; Travkin et al., 1999):

$$f_f = \left[\frac{2 \langle m \rangle \Delta p}{\rho_f \tilde{U}^2 S_w L_x} \right],$$

where \tilde{U} is the average interstitial bulk velocity estimated for the volume where heat transfer occurs. The pumping power per unit volume for a heterogeneous media is given by the following:

$$P_p = \frac{P}{\Omega} = \frac{\dot{m} \Delta p}{\rho_f \Omega} = f_f \text{Re}_{por}^3 \langle m_{yx} \rangle \left(\frac{S_w^4}{\langle m \rangle^4} \right) \frac{\mu^3}{128 \rho_f^2} \left[\frac{W}{m^3} \right],$$

where

$$\langle m_{yz} \rangle = \frac{S_{yz}}{L_y L_z}, \quad L_z = H,$$

and can be seen to be quite different from the expression usually used for a homogeneous media (Andrews and Fletcher, 1996):

$$P_{pm} = \frac{P}{\Omega} = f_f \text{Re}_{por}^3 \wedge f_f^{1/3} \text{Re}_{por}.$$

The factor $\langle m_{yx} \rangle \left(\frac{S_w^4}{\langle m \rangle^4} \right) \mu^3 / (128 \rho_f^2)$ resulting from the VAT based treatment to obtain an expression for a heterogeneous media formula for pumping power can be associated with the morphological influence

$\langle m_{yx} \rangle \left(\frac{S_w^4}{\langle m \rangle^4} \right)$ and with the physical characteristics of the cooling fluid $\mu^3 / (128 \rho_f^2)$.

A second, but more important characteristic to evaluate the heat exchange device, is the heat transfer rate $H_r = (S_{all} \alpha_w^*) / \Omega$ for a known heat flux q_w through the bottom surface of heterogeneous volumetric devices used as heat exchangers

$$H_r = \frac{S_{all} \alpha_w^*}{\Omega} = Nu_w \frac{k_f S_w}{4 \langle m \rangle} S_w^*, \left[\frac{W}{m^3 K} \right],$$

from which the Nusselt number can be found. The Nu_w here is not an internal porous medium heat transfer Nusselt number. It is the bottom wall Nusselt number averaged across both phases. Implicitly it is - the overall (bottom and internal surface) Nusselt number

$$Nu_w = \frac{q_w d_{por}}{(T_{wmax} - T_{in}) k_f}.$$

Not only the effects of combined heat transfer from bottom surface and from within the fins internal volume is responsible for high numbers of Nu_w , as we see below. It is as high as $80 < Nu_w < 800$ in the work by You and Chang (1997), who developed the same idea with only the temperature difference being used being different. They used averaged temperatures for both the bottom surface and internal air temperature.

The ultimate parameter for most kinds of heat exchangers is the ratio of energy transfer rate to pumping power, H_r / P_p , which is the effectiveness of heat transfer per unit volume per unit temperature difference. For a heterogeneous volumetric two-scale heat transfer device it is:

$$E_{eff1} = \frac{H_r}{P_p} = \left[\frac{Nu_w}{f_f Re_{por}^3} \left(32 \frac{S_w^* \langle m \rangle^3}{\langle m_{yz} \rangle S_w^3} \right) \frac{k_f \rho_f^2}{\mu^3} \right], \left[\frac{1}{K} \right],$$

which is distinguished from other expressions for effectiveness by the factor:

$$\left(32 \frac{S_w^* \langle m \rangle^3}{\langle m_{yx} \rangle S_w^3} \right) \left(\frac{k_f \rho_f^2}{\mu^3} \right)$$

The effectiveness number E_{eff1} has been explicitly used for comparison of our four sink samples. Among parameters in the E_{eff1} expression, S_w^* [$1/m$] is the overall specific surface in the volume of heat exchange - including internal surface area, S_{wint} , and bottom wetted surface area, S_{wb} .

The low-speed wind tunnel with an open circuit design is composed of the following sections: (a) an inlet section that includes flow conditioners like flow straighteners and turbulence control screens; (b) a contraction cone or nozzle that accelerates the flow; (c) test section that contains the model to investigate; (d) a diffuser that reduces the air speed

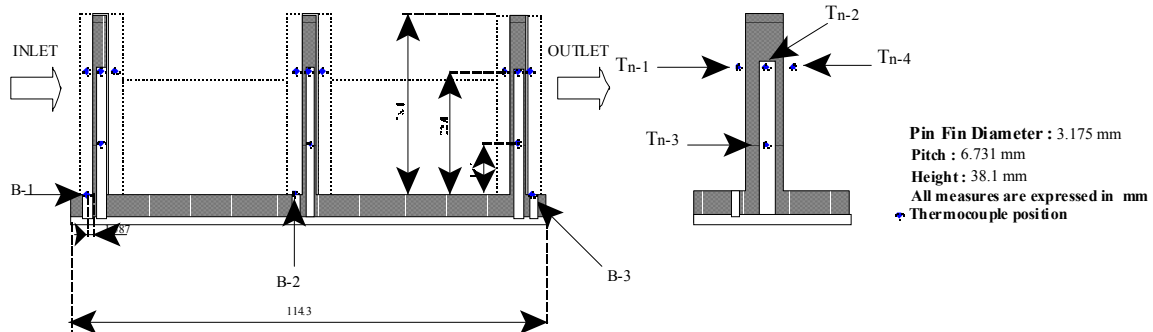


Figure 2 Thermocouple locations inside and outside of pin fins

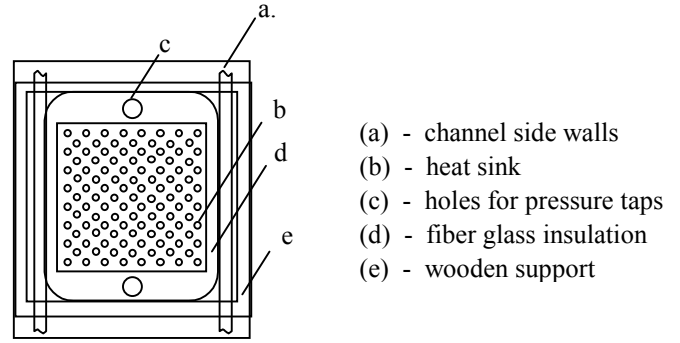


Figure 1 Top view of pin fin heat sink fixture

with as little energy loss as possible; (e) a fan driven by a split capacitor motor that is controlled by an AC-V fan speed control. The wind tunnel is operated in the suction mode; i.e., the fan sucks atmospheric air through the fin assembly and the test section via the bell-mouthed entrance section, with the fan and motor assembly on the exhaust side of the system.

The overall pressure drop through the heat sink is obtain via two static-pressure taps located at the bottom of the test section. A standard differential pressure gage is used. In order to evaluate the velocity profile and the flow rate, velocity measurements were carried out using an air velocity transducer of cylindrical shape, which is inserted from the side walls of the test section Fig. 1. Measurements were taken upstream and downstream of the surface to be tested.

The heat generating source plays an important role in the design of the experimental setup. It serves as a heat source in order to investigate the heat transfer to the environment and pressure loss characteristics of the augmented surface. Three cartridge heaters rated 250 W each were inserted into a copper block with the same area as the heat sinks (114.3mm by 114.3mm) and a thickness of 25,4 mm.

An estimation of the losses through the sides of the wooden box using thermocouples located on each side of the wooden box. The heat sink to be tested is mounted on the copper block.

Under all the test conditions employed, more than 98% of the heat generated in the copper block passed, through the finned heat sink, to the air in the wind tunnel duct. The whole heater box is such that it can be taken apart and assembled easily in few minutes. Temperatures of the copper block were taken by an array of three K thermocouples; temperature profile of the heat sink base was provided by an array of three J

thermocouples located along the air flow direction. To apply the corresponding VAT simulation techniques, temperatures along the pin fins were taken. For each of three pin fins of the heat sink along the flow direction, temperatures forward and backward were measured. Furthermore, the same pin fins were drilled to allow the collocation of two wires in order to measure the pin fin temperature at 1/3 and 2/3 of its height. The same technique was used for longitudinal fins sink – Figs. 2-3. Three narrow channels were grooved at the bottom of the aluminum heat sinks in order to guide the thermocouples out of the heat sink without affecting the surface contact between the aluminum heat sink and the copper block. The narrow channel, where the thermocouple wires were inserted, were then filled with high-conductivity thermal paste. This solution does not affect the air flow pattern into the heat sink. J thermocouples of 0.005” in diameter were used. The inlet and the outlet airstream temperatures in the wind tunnel duct were measured using a thermocouple located at the tip of the anemometer probe. Mapping the velocity profile a map of the temperature distribution is also done. Every thermocouple was calibrated before being installed.

The heat dissipating enhanced surfaces of pin fins samples is made of aluminum with a conductivity of 225 [W/m K], while the longitudinal fins sink has conductivity 204 [W/m K]. Each of the three pin fin heat sinks had constant fin height 0.0381m, constant fin diameter 0.00318m, but the pitch was varied. All the three pin fin heat sinks tested had a *staggered* pin fin layout (Fig. 1).

The series of experiments were initiated with the fin array #1, corresponding to a P/d = 3. The all heat sinks were tested with NO-BYPASS set up. At steady state conditions, pressure drop and temperature were recorded. For the same input power, four different velocities were tested. Every time the steady state was assured before data was collected. The procedure was then repeated for input powers of 50, 125 and 222 W. For every heat sink 12 data points have been taken. The different parameters and their values for pin fin sinks

studied in this investigation are given in Table 1. The repeatability of the experiment was demonstrated by repeat testing.

Table 1 Pin Fins Sinks Parameter and their values

PARAMETER	VALUE
Diameter pin fin	0.3175 cm
Height pin fin	3.81 cm
Pitch h.s. staggered array #1	0.9525 cm
Pitch h.s. staggered array #2	0.71425 cm
Pitch h.s. staggered array #3	0.47625 cm
Heat input, Q_{in}	50,125,222W
By-pass	No
Re_{por}	500 ÷ 20000

For more detail on experiment set up and measurement techniques see Rizzi et al. (2001). For the four samples of sink studied with the results depicted in Figs. 4-12. P_p was measured with a very broad range of Reynolds number $400 < Re_{por} < 17000$.

The samples studied show a consistent pattern of declining friction factor f_f with increasing porous media Reynolds number Re_{por} , see Fig. 4. Some of the observed wavy like fluctuations of f_f were measured in other studies of cross-flow in tube bundles, see Zhukauskas chapter in Heat Exchangers Design Handbook (1983). The range of measured Fanning friction factor $0.45 < f_f < 0.8$ in Fig. 4 compares well with other well known correlations for Fanning friction factor in this range of Reynolds number defined using the VAT formulation (Travkin and Catton, 1998).

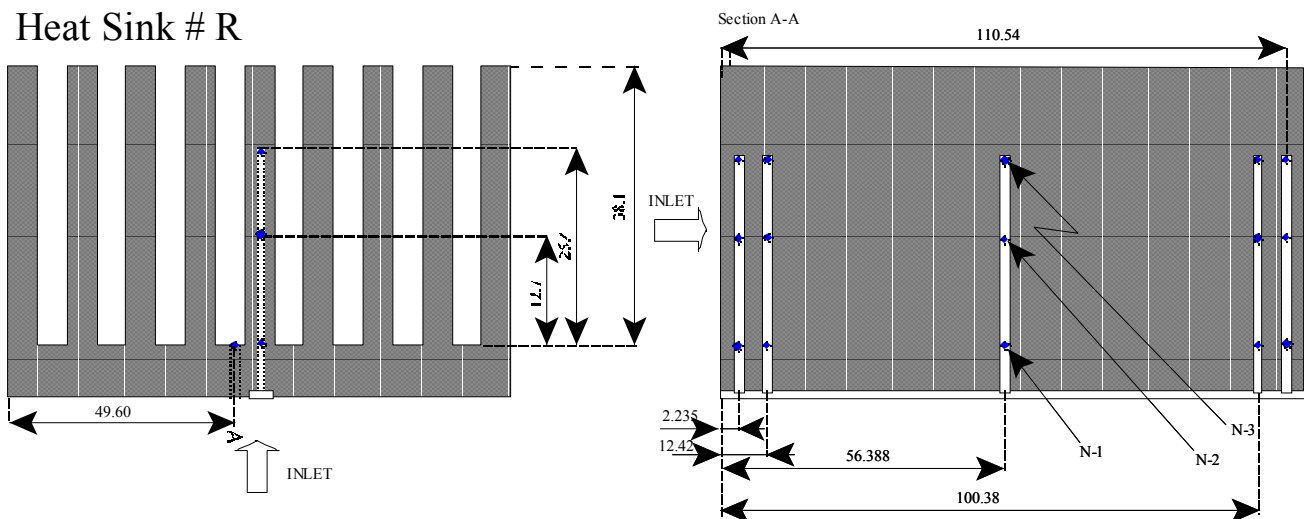


Figure 3 Longitudinal heat sink #R cross-sections and thermocouple locations

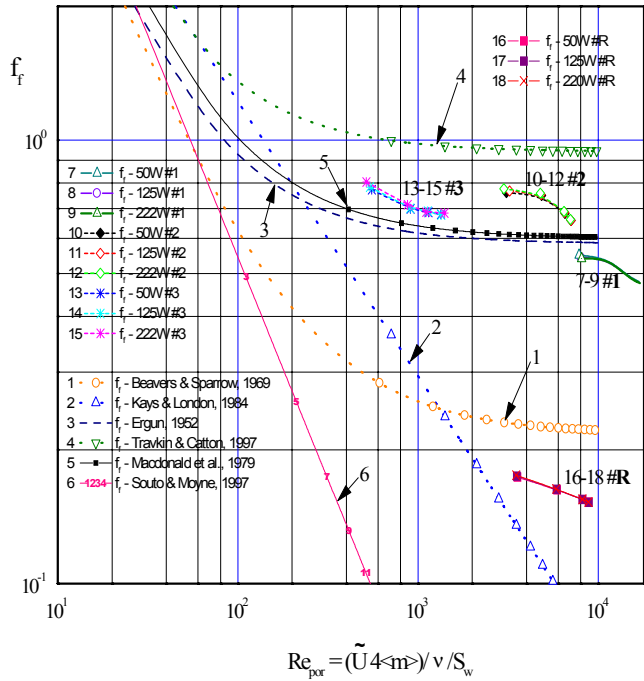


Figure 4 Fanning friction factor f_f (bulk flow resistance in SVAT for different media morphologies, materials and scales used), reduced based on VAT scale transformations in experiments by: 1) Beavers and Sparrow (1969); 2) Kays and London (1984); 3) Ergun (1952); 4) (Travkin and Catton, 1997); 5) Macdonald et al. (1979); 6) Souto and Moyne (1997); 7-9) sink #1; 10-12) sink #2; 13-15) sink #3; 16-18) longitudinal fins sink.

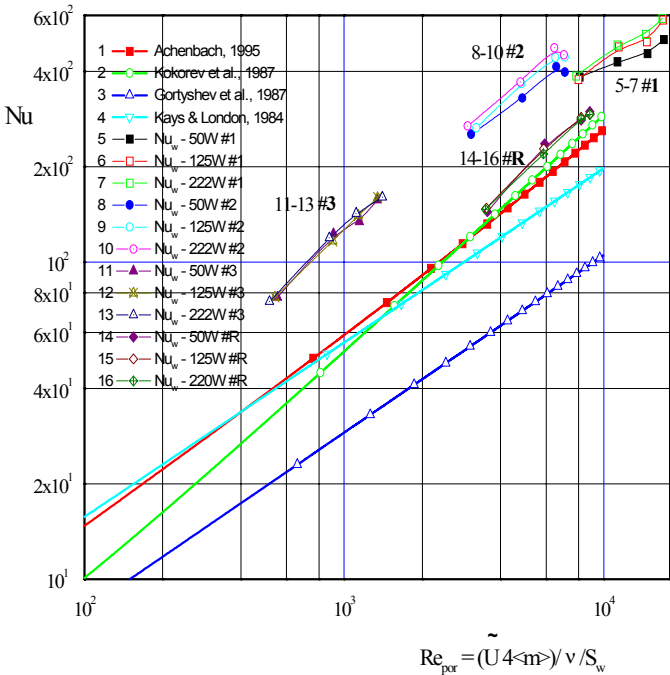


Figure 5 Internal effective heat transfer coefficient in porous media, reduced based on VAT scale transformations in experiments and analysis by: 1) Achenbach (1995); 2) Kokorev et al. (1987); 3) Gortyshov et al. (1987); 4) Kays and London (1984); 5-7) sink #1; 8-10) sink #2; 11-13) sink #3; 14-16) sink #R

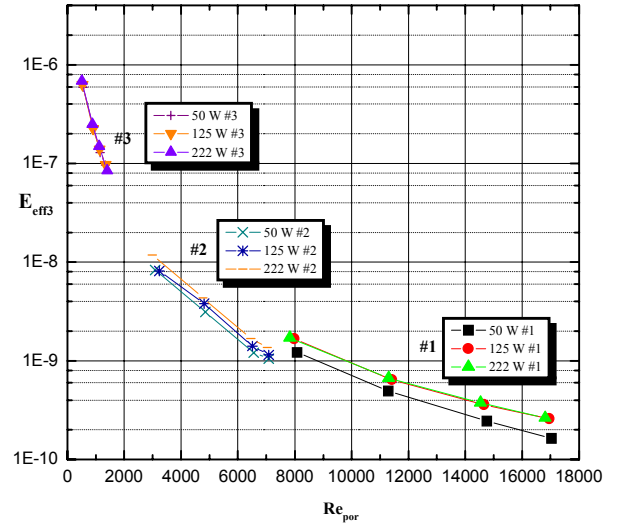


Figure 6 Homogeneous Effectiveness $E_{eff3}(Re_{por})$ for three pin fin heat sinks

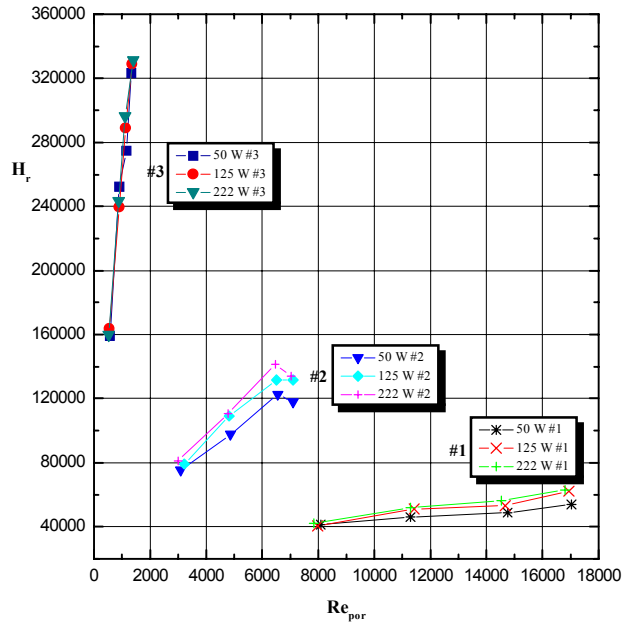


Figure 7 Heterogeneous bulk one-phase heat transfer rate $Hr(Re_{por})$ for three pin fin heat sinks

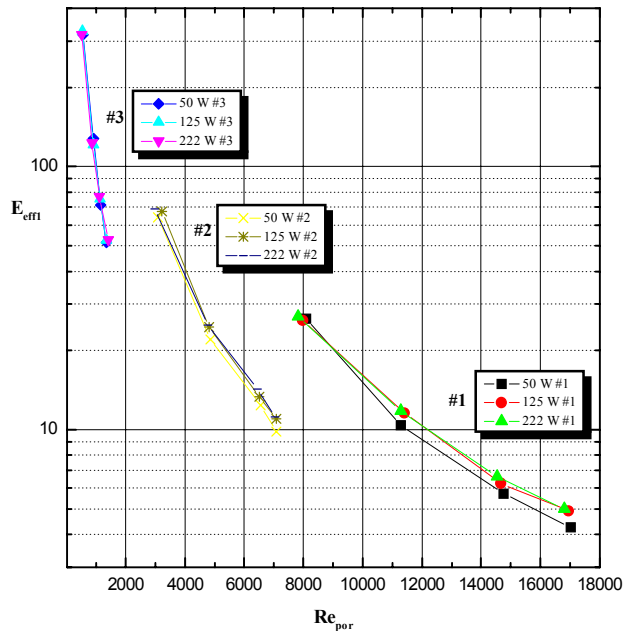


Figure 8 Heterogeneous bulk Effectiveness $E_{effl}(Re_{por})$ for three pin fin heat sinks

Travkin and Catton (1998) and Travkin et al. (1999) recalculated a number of results found in the literature using the VAT based formulae, see Fig. 5, and found substantial differences for this kind of combined heat transfer in comparison to internal media heat transfer coefficient correlations.

Also, the heat transfer rate, H_r (Fig. 7) and the Nusselt number (Fig. 5) curves, for all experiments ($4 \times 12 = 48$), are different and dependent on the bottom heat flux q_w . A great deal of effort was expended to assure ourselves that what was measured was real. Thus, this result does not confirm the assertion by You and Chang (1997) of heat flux independence. Further attention will be given to this result before a strong conclusion will be derived.

Fig. 8 presents measurements of the effectiveness based on the heterogeneous formulation of E_{effl} and Fig. 6 shows its counterpart based on the homogenous formulation. The conclusion drawn from these figures is that the three investigated versions of the same morphology have different effectiveness in different ranges of momentum intensity (Re_{por}). The primary difference between the two figures is the scale. The effectiveness defined using the VAT formulation, however, is much richer in that it contains the parameter dependence of lower scale on upper scale, which the homogeneous formulation cannot.

Compare the two kinds morphology of semiconductor heat sink it is possible to make preliminary observation based on the Figs. 4-8 that the third pin fins sample with more dense packing of fins is the most effective among all four.

This conclusion is not available to reach if one could have the homogeneous characteristics of Figs. 5, 6 because they contradict one to another - Fig. 5 suggests that the best among these three samples is the sample #1. Meanwhile, compare effectiveness in Fig. 6 we can see that the most effective is the sample #3. In our application the most important is the

characteristic of how much energy can be transported outside of the heat sink, but not the amount of energy used for this.

Based on these reasonings designer can compromise in a favor of heat sink #1, which is the least effective, but can withdraw the largest amount of heat in accordance with Nu_w in Fig. 5. This decision can be justified only when the volume of device is not an issue, which usually untrue.

Otherwise, comparing curves in Fig. 7 for the heat transfer rate per unit volume designer would see that the sample #1 is not only the least effective, but can dissipate the smallest amount of heat per unit volume of heat exchanger. That might be the decisive observation.

Also, the homogeneous effectiveness formula curves in Fig. 6 look like they are ready to be used for integration of all three pin fins sinks effectiveness data via approximation of the data by one curve. This could be inappropriate data reduction move according to heterogeneous scaling results of Fig. 8.

There are still insufficiencies in the applied above performance characteristics and some of them would be improved further.

Heterogeneous Two-Scale Two-Phase VAT Analysis of Semiconductor Heat Sinks Experimental Data

Because in the only obtained above criteria all belongs and take into account the characteristics of fluid (convective) heat transfer, and not even one coefficient used explicitly which describes the solid phase characteristics we introduce the heat transfer rate in the solid phase of heat sink as

$$H_{rs} = \frac{S_{ws} \bar{\alpha}_{int}}{\Omega} = \frac{S_{ws} q_s}{\Omega(T_{wmax} - T_{in})} = Bi \left(\frac{k_s S_{ws}}{d_{por} \Omega} \right),$$

$$Bi = \frac{\bar{\alpha}_{int} d_{por}}{k_s}, S_{ws} \neq S_{wint},$$

where S_{ws} characterizes the internal surface of the heat sink, as well as the heat transfer rate for convective heat exchange for the base flat surface minus the area S_{wb} occupied by fins

$$H_{r,bf} = \frac{S_{wb} q_w}{\Omega(T_{wmax} - T_{in})} \left[\frac{W}{m^3 K} \right].$$

These two parameters as shown in our data reduction calculations are much more realistic in terms of energy balance conservation. The amount of heat, for example, dissipated through the fins P_{fins} and the complimentary amount of heat P_{bf} which went to air through the bottom plate of sink #R were compounding to the balances which were less than 5-10% different from the actually produced power by electrical heater.

Accounting for the heat losses in the device and inaccuracy of measuring instruments this is a perfect balance match. Further, as one would note that the primary assigning parameter in experiments is the pumping power per unit volume P_p which was used to set up the comparable conditions for different sinks and regimes. This parameter as independent variable is much better ground for comparison of different devices with different conditions as seen in Figs. 9-12 where all the sinks performance results are exposed more obviously

for deriving conclusions. For example, the homogeneous effectiveness E_{eff3} curves for pin fin sink #2 and longitudinal sink #R in Fig. 10 are located as the sink #R is slightly better performer than sink #2.

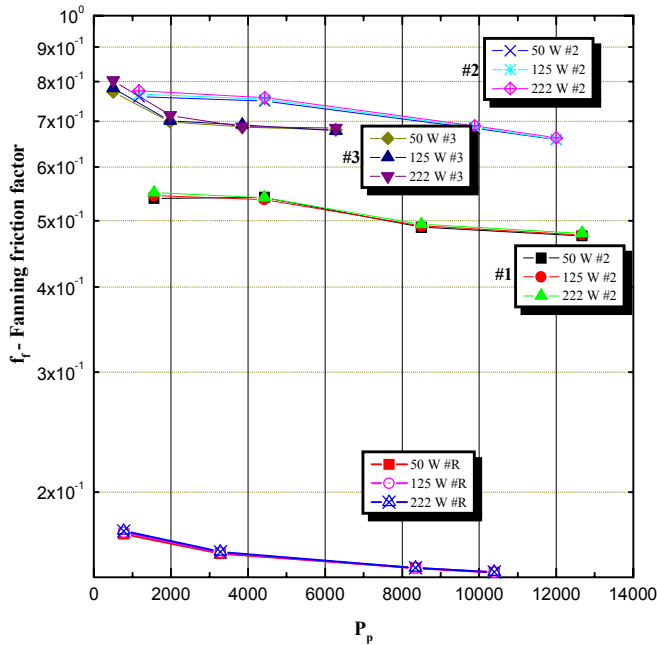


Figure 9 Fanning friction factor $f_f(P_p)$, momentum resistance for all four types of heat sinks

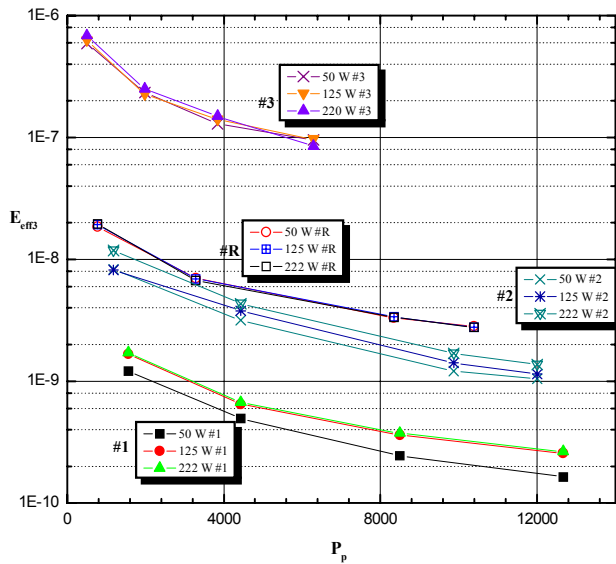


Figure 10 Homogeneous effectiveness parameter $E_{eff3}(P_p)$ for all four types of heat sinks

Accounting for the heat losses in the device and inaccuracy of measuring instruments this is a perfect balance match. Further, as one would note that the primary assigning parameter in experiments is the pumping power per unit volume P_p which was used to set up the comparable conditions for different sinks and regimes. This parameter as independent variable is much better ground for comparison of different

devices with different conditions as seen in Figs. 9-12 where all the sinks performance results are exposed more obviously for deriving conclusions. For example, the homogeneous effectiveness E_{eff3} curves for pin fin sink #2 and longitudinal sink #R in Fig. 10 are located as the sink #R is slightly better performer than sink #2.

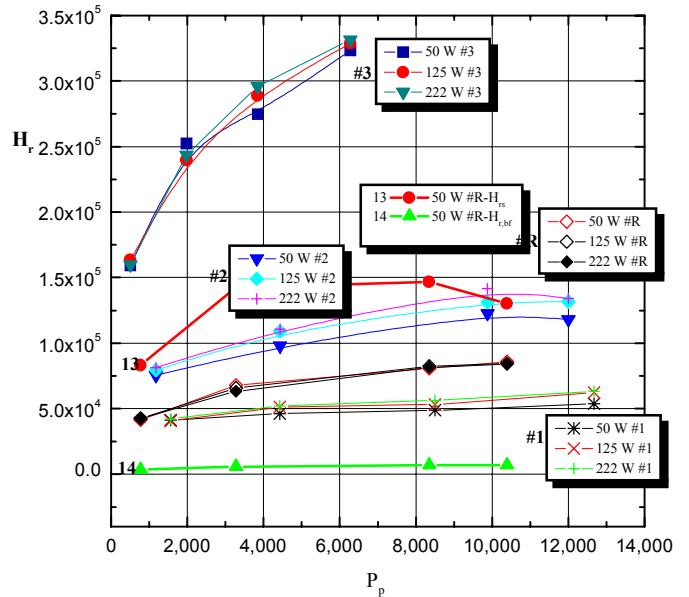


Figure 11 One-phase bulk heat transfer rate $H_r(P_p)$ for all four types of sinks, solid phase heat transfer rate $H_{rs}(P_p)$ and bottom surface (minus fins occupied area) fluid phase heat transfer rate $H_{r,bf}(P_p)$ in experiments with heat sink #R

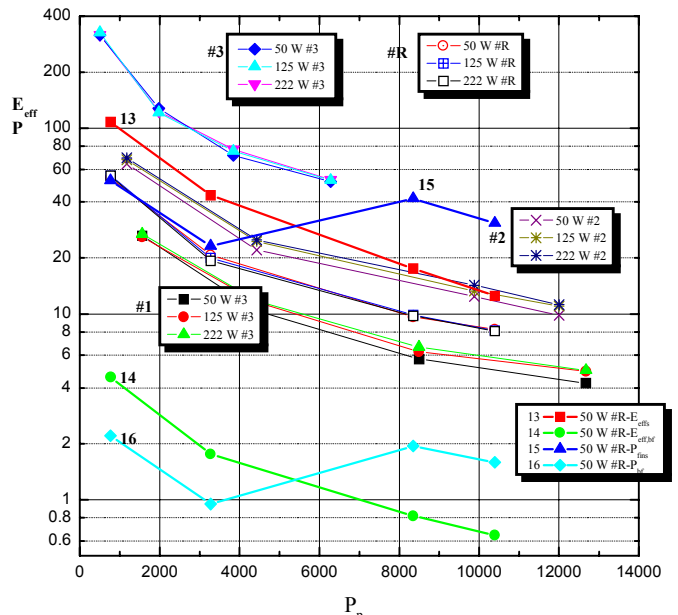


Figure 12 One-phase bulk heterogeneous effectiveness $E_{eff1}(P_p)$ for four types of heat sinks as well as solid phase effectiveness $E_{effs}(P_p)$ and bottom surface (minus fins occupied area) fluid effectiveness $E_{eff,bf}(P_p)$ and dissipated through fins $P_{fins}(P_p)$ and bottom surface $P_{bf}(P_p)$ amount of heat in experiments with heat sink #R

But observation of Figs. 11,12 makes clear that the sink #2 is better in this range of P_p and more of that, the sink #2 probably reaching its maximum of performance approximately at $P_p = 10^4$.

There are the phase based definitions of the effectiveness parameters of solid phase $E_{\text{effs}}=H_{\text{rs}}/P_p$ and the bottom flat surface fluid phase effectiveness $E_{\text{eff,bf}}=H_{\text{rbf}}/P_p$ - Figs. 11,12. These parameters are accurate in the power balance calculations and are directly involved in the VAT mathematical governing equations modeling in a simple way as is the heat sink problem in the flat channel.

Explaining further the variables and definitions used in this two-scale two-phase heterogeneous experimental data reduction procedures we would like to return to published in 1992, 1995 works (Travkin and Catton, 1992, 1995) where the model for analogous problem of turbulent heat transfer in a flat channel filled with porous medium was used. There are eight nondimensional Medium Specific Control Functions (MSCF) or parameters for turbulent regime (Travkin et al., 2000) on the upper scale

$$1) \text{Re}_{mf} = \frac{u_m d_{por}}{\nu}, 2) f_f, 3) m_0, 4) \alpha_T^*,$$

$$5) L_{P7N} = \frac{Pe_m \alpha_T^*}{A_k \left(\frac{1-m_0}{m_0} \right)}, 6) \frac{\tilde{K}_m}{K_b}, 7) \frac{A_k}{Pe_m},$$

$$8) Pe_{TB} = \frac{u_m d_{por}}{a_{TB}}, u_m^2 = - \frac{d_{por}}{\rho_f} \frac{d\langle \bar{p} \rangle}{dx} f,$$

$$Pe_m = \frac{u_m d_{por}}{a_f}, A_k = \frac{k_s}{k_f},$$

and six laminar regime parameters

$$1) \text{Re}_{mf} f_f, 2) \frac{\text{Re}_{mf}}{m_0}, 3) Pe_m, 4) \alpha_L^*,$$

$$5) \frac{\langle sm \rangle}{m_0}, 6) A_k,$$

where a star in α_T^* or α_L^* designates a nondimensional value of internal heat transfer coefficient in porous medium, a_{TB} is

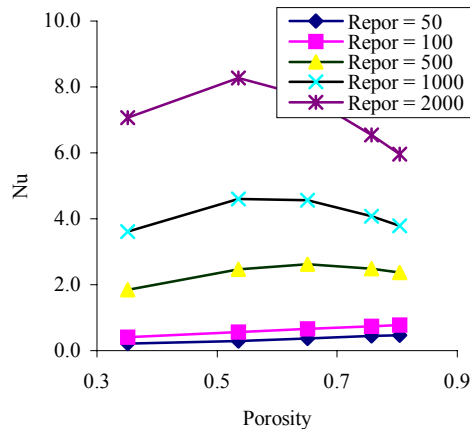


Figure 13 Heat sink bottom wall Nusselt number when changing heat sink porosity.

the turbulent heat diffusivity coefficient at the boundary porous layer-solid phase, \tilde{K}_m , and K_b are the averaged turbulent eddy viscosity and the turbulent kinetic energy exchange coefficient. It can be shown that the heat transfer rate H_r and effectiveness parameter E_{effs} can be derived in the VAT governing equations with nondimensional parameters shown above when the whole volume of heat sink is presented as the representative elementary volume (REV).

Meanwhile, the parametric studies of heat sink performance optimization (Travkin et al., 2000, 2001) revealed in a more obvious way that the sink's heat exchange rate or effectiveness maximization is the real multidimensional problem, but not only a dependency on Re_{por} , f_f or heat exchange coefficients.

As depicted in Fig. 13 the heat sink Nusselt number for one of simulated sinks varies for different porosity and different pore Reynolds number. It is obvious that Nusselt number is high when Reynolds number is high. For high Reynolds number, heat transfer performance will be best at certain Reynolds numbers.

The next logical step in obtaining the better performance characteristics for volumetric heat dissipative device is to consider the whole number of effects which participate in momentum and heat transport in a bulk heterogeneous volume. Thus, in the momentum equation those are convective and diffusive heterogeneous fluctuations transport terms in governing equations. In fluid temperature equation, for example, those are the terms with convective fluctuations transport and two terms with surficial effect of inhomogeneous temperature of interface. All of these four terms need to be added to conventional heat flux via interface exchange term (Travkin et al. 2000).

The more complete parameters set for the heat exchange rate, pumping power per unit volume and effectiveness were considered in their full forms.

Conclusions

While considering the problem of experimental set-ups and experimental data reduction for the two-scale semiconductor heat sink, a number of new criteria for momentum and heat transport were derived to connect the local and overall (as temperature in inlet and outlet, etc.) characteristics to the parameters of VAT scaled models. The reason for heterogeneous parameter usage is shown while accomplishing the analysis of the experimental results for heat sink performance – it yields a better, more exact description of the influence of the media and both phase characteristics on transport values.

These parameters are so specific that they allow one to distinguish the input of any mechanism or mode of heat transfer occurring in the device. The heat transfer device is presented as two-scale local- non-local heterogeneous heat exchanger with controls on both scales. For example, the heat transfer rates and effectiveness formulated for both phases which improve the energy balance assessment.

We have outlined the consequences of the experimental procedures and design, because the larger number of influencing phenomena make possible the larger number of

choices in optimization of performance or in increasing the heat exchange rate to its possible highest level. The latter is the goal of preference in cooling of semiconductor devices.

Experimental results were simulated using non-local VAT model and also compared to a number of works in the area of heat sink design and simulation.

Acknowledgments

This work was partly sponsored by the Department of Energy, Office of Basic Energy Sciences through the grant DOE-FG03-89ER14033 A002. And partly sponsored by the DARPA grant.

References

Andrews, M.J. and Fletcher, L.S., "Comparison of Several Heat Transfer Enhancement Technologies for Gas Heat Exchangers," *J. Heat Transfer*, Vol. 118, pp. 897-902, 1996.

Bejan, A. and Morega, A.M., "Optimal Arrays of Pin Fins and Plate Fins in Laminar Forced Convection," *J. Heat Transfer*, Vol. 115, pp. 75-81, 1993.

Bejan, A., "The Optimal Spacing for Cylinders in Crossflow Forced Convection," *J. Heat Transfer*, Vol. 117, pp. 767-770, 1995.

Fabbri, G., "Optimum Performances of Longitudinal Convective Fins with Symmetrical and Asymmetrical Profiles," *Int. J. Heat Fluid Flow*, Vol. 20, pp. 634-641, 1999.

Jubran, B.A., Hamdan, M.A., and Abdualh, R.M., "Enhanced Heat Transfer, Missing Pin, and Optimization for Cylindrical Pin Fin Arrays," *J. Heat Transfer*, Vol. 115, pp. 576-583, 1993.

Kim, S.J. and Kim, D., "Forced Convection in Microstructures for Electronic Equipment Cooling," *J. Heat Transfer*, Vol. 121, No.3, pp. 639-645, 1999.

You, H.-I., and Chang, C.-H., "Numerical Prediction of Heat Transfer Coefficient for a Pin-Fin Channel Flow," *J. Heat Transfer*, Vol. 119, No. 4, pp. 840-843, 1997.

Bejan, A. and Sciubba, E., "The Optimal Spacing of Parallel Plates Cooled by Forced Convection," *Int. J. Heat Mass Transfer*, Vol. 35, No. 12, pp. 3259-3264, 1992.

Bejan, A., "Constructal Trees of Convective Fins," *J. Heat Transfer*, Vol. 121, pp. 675-682, 1999.

Vafai, K. and Tien, C.L., "Boundary and Inertia Effects on Flow and Heat Transfer in Porous Media," *Int. J. Heat and Mass Transfer*, Vol. 24, pp. 195-203, 1981.

Rizzi, M., Canino, M., Hu, K., Jones, S., Travkin, V.S., and Catton, I., "Experimental Investigation of Pin Fin Heat Sink Effectiveness," accepted for ASME-NHTC'2001.

Beavers, G.S. and Sparrow, E.M., "Non-Darcy Flow Through Fibrous Porous Media," *J. Applied Mechanics*, Vol. 36, pp. 711-714, 1969.

Kays, W.M. and London, A.L., *Compact Heat Exchangers*, 3rd ed., McGraw-Hill, New York, 1984.

Ergun, S., "Fluid flow through packed columns," *Chemical Engineering Progress*, Vol. 48, 89-94, 1952.

Travkin, V.S. and Catton, I., Homogeneous and non-local heterogeneous transport phenomena with VAT application analysis, in *Proc. 15th Symposium on Energy Engineering*

Sciences, Argonne National Laboratory, Conf. - 9705121, pp. 48-55, 1997.

Macdonald, I.F., El-Sayed, M.S., Mow, K., and Dullien, F.A.L., "Flow through Porous Media - the Ergun Equation Revisited", *Ind. Eng. Chem. Fundam.*, Vol. 18, No. 3, pp. 199-208, 1979.

Souto, H.P.A. and Moyne, C., "Dispersion in two dimensional periodic porous media. Part I. Hydrodynamics. Part II. Dispersion Tensor", *Phys. Fluids*, Vol.9, No.8, p2243-2263, 1997.

Achenbach, E., "Heat and Flow Characteristics in Packed Beds," *Experimental Thermal and Fluid Science*, Vol. 10, pp. 17-21, 1995.

Kokorev, V. I., Subbotin, V. I., Fedoseev, V. N., Kharitonov, V.V., and Voskoboynikov, V.V., "Relationship Between Hydraulic Resistance and Heat Transfer in Porous Media," *High Temperature*, Vol. 25, No. 1, pp. 82-87, 1987.

Gortyshov, Yu.F., Muravev, G.B., and Nadyrov, I.N., "Experimental Study of Flow and Heat Exchange in Highly Porous Structures," *Engng.-Phys. Journal*, Vol. 53, No. 3, pp. 357-361, (in Russian), 1987.

Gratton, L., Travkin, V.S., and Catton, I., "The Influence of Morphology upon Two-Temperature Statements for Convective Transport in Porous Media," *J. Enhanced Heat Transfer*, Vol. 3, No. 2, pp.129-145, 1996.

Travkin, V.S., Gratton, L., and Catton, I., "A Morphological-Approach for Two-Phase Porous Medium-Transport and Optimum Design Applications in Energy Engineering," in *Proc. Twelfth Symposium on Energy Engineering Sciences*, Argonne National Laboratory, Conf. -9404137, pp. 48-55, 1994.

Travkin V. S. and Catton, I., "A two temperature model for turbulent flow and heat transfer in a porous layer," *Advances in Colloid and Interface Science*, Vol. 76-77, pp. 389-443, 1998.

Travkin, V.S. and I. Catton, "Compact Heat Exchanger Optimization Tools Based on Volume Averaging Theory," in *Proc. 33rd ASME NHTC, NHTC99-246*, ASME, New Mexico, 1999.

V.S. Travkin, I. Catton, K. Hu, A.T. Ponomarenko, and V.G. Shevchenko, "Transport Phenomena in Heterogeneous Media: Experimental Data Reduction and Analysis", in *Proc. ASME, AMD-233*, Vol. 233, pp. 21-31, 1999.

Travkin, V.S., Catton, I., and Hu, K., "Optimization of Heat Transfer Effectiveness in Heterogeneous Media," in print in *Proc. of the Eighteenth Symposium on Energy Engineering Sciences*, Argonne National Laboratory, 2000.

Travkin, V.S. and Catton, I., "Models of Turbulent Thermal Diffusivity and Transfer Coefficients for a Regular Packed Bed of Spheres", in *Fundamentals of Heat Transfer in Porous Media*, ASME HTD-Vol. 193, pp.15-23, 1992.

Travkin, V.S., and Catton, I., "A Two-Temperature Model for Turbulent Flow and Heat Transfer in a Porous Layer", *J. Fluids Engineering*, Vol. 117, pp. 181-188, 1995.

Travkin, V.S., Hu, K., and Catton, I., (2001), "Multi-variant Optimization in Semiconductor Heat Sink Design," accepted for ASME-NHTC'2001.